# Evaluating the Performance of Turbo Codes and Turbo-Coded Modulation in a DS-CDMA Environment

Volker Kühn
University of Bremen (Germany)
Department of Telecommunications
Kufsteiner Strasse NW 1
D-28359 Bremen
e-mail: kuehn@comm.uni-bremen.de

*Abstract*— ***Recently, turbo codes have received great attention due to their outstanding performance. Unfortunately, a high performance is associated with large transmission delays prohibiting an application for speech transmission. Hence, the aim of this paper is the comparison of turbo codes employing short interleavers with convolutional codes in terms of bit error rate performance and computational effort. Additionally, a pragmatic approach of bandwidth-efficient turbo-coded modulation is considered. Analyzing the structure of transmitter and receiver interesting results are presented concerning the design of the mapper. Furthermore, a new very simple soft-output demodulation algorithm is derived.***

***In order to compare turbo codes with convolutional codes under realistic conditions, both are embedded in a DS-CDMA system. Besides this comparison a compromise between a high coding gain (low code rate) and high Direct-Sequence spreading is worked out including the consideration of the turbo-coded modulation scheme. Simulation results indicate that turbo codes with small block interleavers do not outperform conventional convolutional codes. Furthermore, it is shown that for coherent demodulation low code rates and low DS-spreading is superior to high code rates and high DS-spreading.***

*Keywords*— ***CDMA, turbo codes, turbo coded modulation***

## I. Introduction

SINCE turbo codes (TC) were introduced in 1993 [1], plenty of work has been done on analyzing their amazing performance and their limits as well. The great interest in turbo codes is motivated by the fact that they perform near the Shannon limit. Specifically, a lot of investigation has been carried out analyzing both the encoder and the iterative decoding procedure. Meanwhile, many secrets of turbo codes were unveiled, although still a lot of problems remain.

Turbo codes themselves represent a sophisticated continuation of Forney's concatenated codes [2]. They consist of parallel concatenated recursive convolutional codes connected by an interleaver and the overall code rate can be adjusted by puncturing the redundancy bits of each constituent code. In order to find optimal constituent codes an analysis of the distance spectrum of turbo codes supplies design criteria. Concerning the structure of the inherent interleaver, several attempts show significant performance improvements especially for large interleavers. However, the best method for selecting an optimal interleaver design has not been comprehensively proven up to now.

Since maximum likelihood decoding requires high computational costs, a sub-optimum iterative decoding scenario is used. Here, several optimum and sub-optimum soft-in/soft-out decoding algorithms were derived in order to achieve close to optimal performance with acceptable decoding effort [3],[4],[5], [6],[7]. In the meantime, the iterative philosophy itself was embedded in many other environments such as combined equalization and decoding [8].

Furthermore, the combination of turbo codes with bandwidth-efficient modulation, termed turbo-coded modulation, outperforms the classical trellis coded modulation (TCM) of Ungerboeck [9] in terms of the bit error rate. Besides first approaches described in [10],[11] there exist even more sophisticated techniques concatenating TCM-modules in a parallel manner [12],[13], [14],[15].

Regardless of the specific application, reaching the Shannon limit seems to be approachable with very large interleavers only causing tremendous transmission delays and prohibiting an application for speech-transmission. In [16], a gap of only 0.7 dB to Shannon's limit remains when using a random interleaver of $L = 65536$ bits causing a delay of $\tau = 13.65$ s at a data rate of $R_d = 9.6$ kbit/s. This delay comes only from reading and writing the interleaver and does not include the processing delay of transmitter and receiver. Nevertheless, the general concept of concatenated codes in combination with an iterative decoding scheme allows a significant improvement of the performance of modern communication systems. Therefore, it is an important task to investigate whether turbo codes and turbo-coded modulation are still superior to conventional coding concepts under the constraint of moderate interleaver sizes.

The goal of this paper is to compare the performance of turbo codes and conventional convolutional codes under the assumption of approximately equal decoding costs and acceptable equal transmission delays. Besides this comparison, a pragmatic approach of a turbo-coded modulation scheme is analyzed. Here, interesting results concerning the mapping of turbo-coded bits onto channel symbols and a new very simple soft-output demodulation technique are presented. The author uses a Direct-Sequence Code Division Multiple Access (DS-CDMA) system as simulation environment because wideband CDMA is chosen as a multiple access technique for third generation mobile radio systems based on the UMTS standard. The typical CDMA environment is studied in order to find a compromise between DS spreading, channel coding and modulation. Furthermore, the influence of an imperfect channel estimation on the coding gain is investigated. All simulations are restricted to an interleaver size of $L = 400$ bits leading to an inherent delay of about $\tau = 83,3$ ms at a data rate of $R_d = 9.6$ kbit/s. This delay that is complemented by the processing delay of transmitter and receiver seems to be acceptable even for speech transmission. At this point it has to be mentioned that it is not the intention of this paper to investigate the overall performance of a CDMA system taking into account substantial techniques like interference cancellation or power control. These topics may be of interest in a next step.

The paper is organized as follows: Section 2 reviews the general concept of turbo codes, analyzes their distance properties and give some guidelines for optimal generator polynomials. Additionally, the iterative decoding procedure is illustrated briefly. Section 3 describes a turbo-coded modulation scheme [10], explains in detail a pragmatic mapping strategy and derives a low cost demodulation algorithm supplying soft-output values. Section 4 treats the simulation model and Section 5 presents the results.

## II. Turbo Codes

### A. Structure of the Encoder

The structure of the encoder is shown in Figure 1 [16]. Turbo codes are systematic codes consisting of at least two parallel concatenated constituent codes $C_1$ and $C_2$ connected by an interleaver $\Pi$. A code word $\mathbf{c}(k)$ consists of the systematic information bit $d(k)$ and the redundancy bits $\mathbf{c}_1(k)$ and $\mathbf{c}_2(k)$ of the constituent encoders $C_1$ and $C_2$, respectively. The interleaver approximately ensures statistical independence of the parity bits $\mathbf{c}_1(k)$ and $\mathbf{c}_2(k)$ which is an important property for the iterative decoding process. As will be shown in the next section, the interleaver reduces the number of sequences with low Hamming weight ensuring therefore high performance at low signal-to-noise ratios. Assuming identical constituent codes with rates $R_{c1} = R_{c2} = 1/n$, the overall code rate of the unpunctured turbo code is $R_c = 1/(2n-1)$. A larger overall code rate $R_c$ can be realized by puncturing $\mathbf{c}_1(k)$ and $\mathbf{c}_2(k)$ with respect to a matrix $\mathbf{P}$ (for an example see Table I in Section II-C). Each column of $\mathbf{P}$ contains $2(n-1)$ elements associated with the same number of parity bits of the vector $\tilde{\mathbf{c}}(k) = [\mathbf{c_1}(k) \;\; \mathbf{c}_2(k)]^T$. A zero-element in $\mathbf{P}$ indicates that the corresponding bit of $\tilde{\mathbf{c}}(k)$ is not transmitted. The columns are read periodically one after another so that puncturing is performed with a period identical to the number of columns of $\mathbf{P}$.

### B. Analysis of distance spectra

Analyzing the distance properties of a code allows the estimation of the code's performance by appropriate boun-

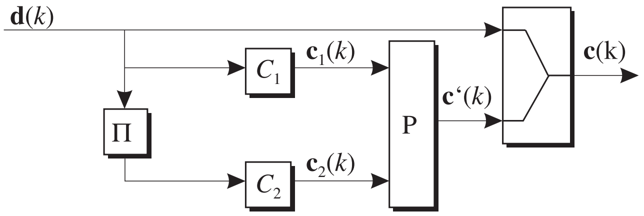


Fig. 1. Structure of the turbo-encoder

ding techniques. In this paper, we follow the derivation given in [17],[18],[19]. Due to the linearity of convolutional codes it is sufficient to compare each sequence with the all-zero-path instead of comparing every sequence with each other. Therefore, only the Hamming weight of sequences in the trellis has to be regarded. If tail bits are appended to the data stream $d(k)$ forcing the encoder to return into the all-zero-state, the convolutional code with a terminated trellis can be interpreted as an equivalent block code of finite length $L$. For such a code, the distance spectrum or transfer function is defined as

$$A(W,C,L,R) = \sum_w \sum_c \sum_l \sum_r A_{w,c,l,r} \cdot W^w \cdot C^c \cdot L^l \cdot R^r \quad (1)$$

where $A_{w,c,l,r}$ denotes the number of path in the trellis with an input weight of $w$, a weight of the redundancy bits of $c$, a total length of $l$ code words and $r$ remergings with the all-zero-sequence. The total weight of a sequence is then given by $d = w + c$. If we sum up all sequences with the same input weight $w$ and redundancy weight $c$ considering all error events of length $l$ and all possible remergings $r$, we get the following expression [17]

$$A_{w,c} = \sum_l \sum_r A_{w,c,l,r} \cdot \underbrace{\begin{pmatrix} L-l-r \\ r \end{pmatrix}}_{K(l,r)} \quad (2)$$

with $K(l,r)$ as the number of possibilities to arrange $r$ sequences of total length $l$ in a frame of length $L$.

Determining the transfer function of the entire turbo code requires now the consideration of the specific interleaver. Until now, there exist no prove for an optimal interleaver design although plenty of work has been spent on this problem. In [17],[18] the use of a *uniform interleaver* is proposed. The uniform interleaver is a theoretical device that represents an average of all possible interleaver structures. In practice, there will be at least one interleaver that performs equal or even better than the average.

It has to be emphasized that both constituent codes $C_1$ and $C_2$ always receive input sequences of equal weight because the interleaver just permutes the input sequence $d(k)$, it does not flip the bits. Thus, it is advantageous to rewrite (2) as a weight enumeration function conditioned on a specific input weight $w$

$$A_w(C) = \sum_c A_{w,c} \cdot C^c. \quad (3)$$

With (3) a good approximation of the conditional weight enumerating function of the turbo code is obtained with the expression [17], [18],[19]

$$A_w^{TC}(C) = \frac{A_w(C) \cdot A_w(C)}{\begin{pmatrix} L \\ w \end{pmatrix}} = \sum_c A_{w,c}^{TC} \cdot C^c. \qquad (4)$$

Due to the multiplication of the transfer functions of each constituent code all possible permutations of the interleaver are taken into account. Hence, the result is an average distance spectrum over all possible input sequences $d(k)$ with weight $w$. The denominator in (4) describes the number of ways to arrange $w$ information bits equal to "1ïn a block of length $L$ and performs a normalization.

Using the distance spectrum in (4) we can approximate easily the bit error rate of a given turbo code with the well-known union bound [20]

$$P_b \leq \sum_{d=d_f}^{\infty} c_d \cdot P_d \qquad (5)$$

with $P_d$ as pairwise error probability of two sequences with Hamming distance $d$. $c_d$ denotes the total weight of information bits for all sequences with Hamming weight $d$ normalized by $L$ and thus represents the average number of bit errors. The coefficients $c_d$ can be obtained by the relation

$$c_d = \sum_w \sum_{c=d-w} \frac{w}{L} \cdot A_{w,c}^{TC}. \qquad (6)$$

For the case of an AWGN channel the pairwise error probability is given by

$$P_d = \frac{1}{2} \cdot \operatorname{erfc}\left(\sqrt{\frac{dR_c E_b}{N_0}}\right) . \qquad (7)$$

Incorporating (6) and (7) in (5) we get the same expression as equation (2) given in [19] where $c_d$ corresponds with the fraction $\frac{N_d \tilde{w}_d}{N}$. For the fully-interleaved frequency nonselective Rayleigh fading channel, $P_d$ has the form [20],[11]

$$P_d = \left(\frac{1-\mu}{2}\right)^d \cdot \sum_{j=0}^{d-1} \begin{pmatrix} d-1+j \\ j \end{pmatrix} \cdot \left(\frac{1+\mu}{2}\right)^j \qquad (8)$$

$$\text{with} \qquad \mu = \sqrt{\frac{E_s/N_0}{1+E_s/N_0}} .$$

Figure 2 depicts in the left diagram the coefficients $c_d$ of a turbo code with an overall code rate $R_c = 1/3$. Two constituent codes with generators polynomials $(1, \frac{1+D^2}{1+D+D^2})$ are employed. The diagram on the right hand side illustrates upper bounds on the corresponding bit error rates. In order to allow a direct comparison with convolutional codes, the distance spectrum of a code with constraint length $L_c = 9$ and rate $R_c = 1/3$ and the appropriate bit error rate are also shown. The large constraint length ensures approximately the same decoding costs for convolutional and turbo code.

Regarding the coefficients $c_d$, it becomes obvious that the number of sequences with a certain total weight occur more seldomly in the case of turbo codes than in the case of convolutional codes. This difference is enlarged with increased interleaver size. In [19] it is shown that high weight sequences dominate the bit error rate at low signal-to-noise ratios in the case of convolutional codes. In contrast, turbo codes show a dominance of the free distance asymptote leading to the superior behavior at low signal-to-noise-ratios as depicted in Figure 2. Even for an interleaver size of $L = 100$ there seems to be a slight advantage of the turbo code for signal-to-noise ratios up to 4 dB. This advantage is increased with a larger interleaver $L = 400$.

In contrast to this, the free distance of the convolutional code ($d_f = 18$) is nearly 2.5 times as high as that for the turbo code ($d_f = 7$) with the uniform interleaver. Hence, the asymptotic coding gain is much higher for the convolutional code as illustrated in the right diagram of Figure 2. Here, the steepness of the BER curves for the convolutional code is much higher for signal-to-noise ratios above 4 dB. Hence, as stated by Perez et al. [21], we know that the free distance $d_f$ of a code is not the critical parameter for reaching Shannon's limit. It is rather necessary to construct codes with extremely few sequences of low weight to perform well for low signal-to-noise ratios.

At this point, it has to be mentioned that the bounding technique used for the discussed results is not very accurate for bit error rates above $P_b > 10^{-2}$ [11]. Additionally, the determination of the distance spectrum causes high computational costs if high weight sequences have to be considered. This effort is even higher when puncturing is applied because puncturing results in time-variant codes. Hence, it is recommendable to use this bounding technique only for low bit error rates where Monte-Carlo simulations are too expensive. For medium range error rates Monte-Carlo simulations are to be prefered.

All results described until now have been achieved with the aid of the uniform interleaver. In general, choosing a specific interleaver structure is a very difficult task because there exist no easy construction guides. The computational effort required for optimizing the interleaver's structure is such high that up to now only incomplete results have been published. Concerning the application of turbo codes for speech transmission, the tolerable transmission delay has to be restricted to approximately 100 ms. For this reason, an interleaver size of $L = 400$ bits is chosen limiting the performance of turbo codes dramatically. Fortunately, for such short block lengths even simple block interleavers show acceptable performance above $P_b = 10^{-4}$ [22]. Therefore, simple block interleavers are employed in this article.

### C. Design Criteria for Optimal Constituent Codes

After presenting a bounding technique and first comparative results for turbo codes and convolutional codes, this section describes some design criteria for constructing good constituent codes. As derived in [17], systematic and re-

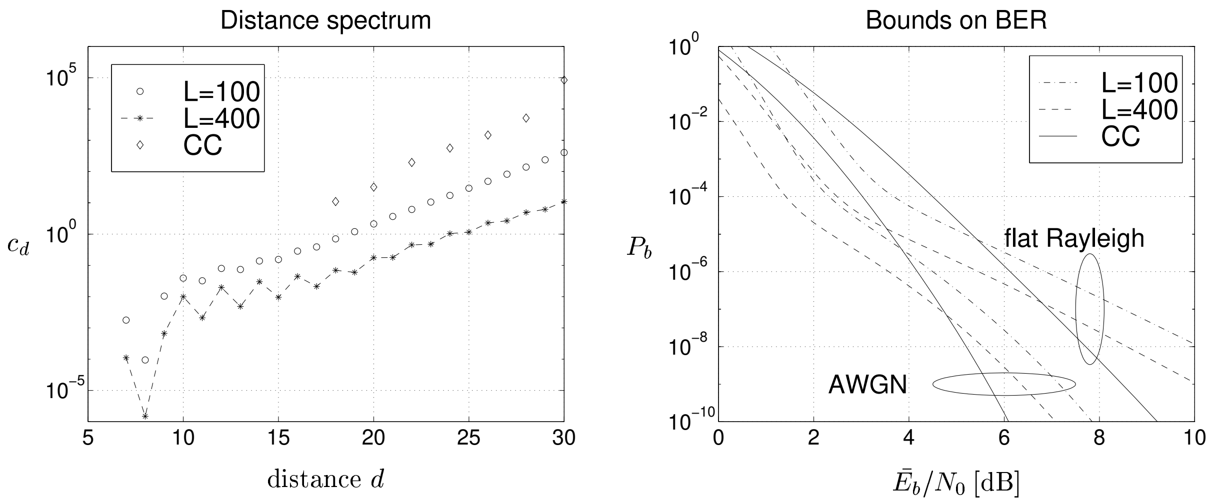


Fig. 2. Distance spectra and bounds on bit error rate for convolutional codes and turbo codes for AWGN and fully-interleaved Rayleigh fading channel

cursive convolutional codes have to be employed in order to take advantage of an increased interleaver size. Furthermore, it is shown in [18] that the effective free distance

$$d_{eff} = 2 + 2 \cdot z_{min} \tag{9}$$

is a critical parameter to be optimized. In (9) $z_{min}$ represents the minimum weight of the redundancy bits of one constituent code $C_i$ for an input weight of $w = 2$. In order to maximize $d_{eff}$, constituent codes with primitive feedback polynomials were chosen because they maximize the minimal length of output sequences for an input weight of $w = 2$. The longer the output sequence for a $w = 2$ input sequence, the higher is the weight of the redundancy bits that can be incorporated into this sequence. Hence, the other polynomials should be selected in a way to maximize the Hamming weight of $\mathbf{c}_i$ with respect to the recursive polynomial. The specific constituent codes and the corresponding puncturing matrices used in this article are given in Table I. The superscript $r$ indicates the recursive polynomial. A list of optimal constituent codes with different constraint lengths can be found in [18].

As shown in Table I, the overall code rates $R_c = 1/2$ and $R_c = 2/3$ are obtained with constituent codes of rate $R_{c1} = R_{c2} = 1/2$ and appropriate puncturing of the redundancy bits. For $R_c = 1/2$, the redundancy bits of both constituent codes are transmitted alternately, whereas for $R_c = 2/3$ only every fourth bit of each encoder is transmitted. The turbo code with $R_c = 1/4$ employs constituent codes of rate $R_{c1} = R_{c2} = 1/3$ each punctured to a code of rate $R_{c1} = R_{c2} = 2/5$.

TABLE I

Generator polynomials for different code rates

| Code rate | CC, $L_c = 9$ | TC, $L_c = 5$ | $\mathbf{P}$ |
|---|---|---|---|
| $R_c = \frac{1}{2}$ | $\mathbf{g}_1 = 561_8$<br>$\mathbf{g}_2 = 753_8$ | $\mathbf{g}_1^r = 23_8$<br>$\mathbf{g}_2 = 35_8$ | $\begin{pmatrix} 1 & 0 \\ 0 & 1 \end{pmatrix}$ |
| $R_c = \frac{1}{4}$ | $\mathbf{g}_1 = 463_8$<br>$\mathbf{g}_2 = 535_8$<br>$\mathbf{g}_3 = 733_8$<br>$\mathbf{g}_4 = 745_8$ | $\mathbf{g}_1^r = 23_8$<br>$\mathbf{g}_2 = 35_8$<br>$\mathbf{g}_3 = 25_8$ | $\begin{pmatrix} 1 & 1 \\ 1 & 0 \\ 1 & 1 \\ 0 & 1 \end{pmatrix}$ |
| $R_c = \frac{2}{3}$ | | $\mathbf{g}_1^r = 23_8$<br>$\mathbf{g}_2 = 35_8$ | $\begin{pmatrix} 1 & 0 \\ 0 & 0 \\ 0 & 0 \\ 0 & 1 \end{pmatrix}$ |

## D. Turbo-Decoder

The last section has analyzed the turbo *encoder* by an appropriate bounding technique. This section gives now a brief description of the turbo *decoder* shown in Figure 3. The two decoders $D_1$ and $D_2$ corresponding to the constituent codes $C_1$ and $C_2$, respectively, are serially arranged and connected by an interleaver. Due to this serial concatenation we refer to decoder $D_1$ as the *inner* decoder and to decoder $D_2$ as the *outer* decoder. The extrinsic information $Z_1(k)$ of the first decoder $D_1$, i.e. the information obtained only from the redundancy bits of $C_1$ [16], can be used as a-priori-information for $D_2$ and vice versa. As a consequence, after de-interleaving $(\Pi^{-1})$ the extrinsic information of $D_2$, $Z_2(k)$ is passed back to $D_1$ and an iterative decoding procedure arises. As the decoding algorithm, the Max-Log-MAP-algorithm is applied [23],[24]. Investigations have shown that this is an appropriate compromise between performance, robustness and computational effort [11].

Assuming approximately twice as high computational costs for iterative soft-in/soft-out decoding of turbo codes in comparison with simple Viterbi decoding of convolutional codes [4], we can run three decoding iterations if a convolutional code with constraint length $L_c = 9$ is considered

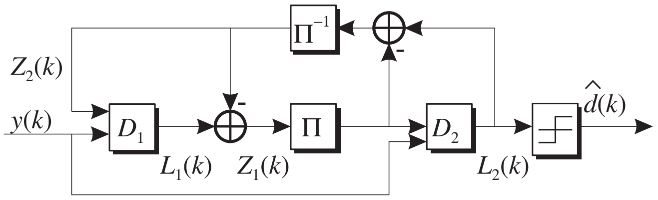


Fig. 3. Structure of turbo-decoder

[1]. The code rate is slightly reduced in case of convolutional coding because more tail bits are needed to terminate the trellis. This disadvantage can be compensated by slightly puncturing the convolutional code with negligible performance loss. The trellis of the first constituent code is always terminated.

Concerning implementation issues, simulation results indicate that the noise power need not to be estimated explicitly. Instead, the constant $\sigma^2 \equiv 0.1$ represents an appropriate choice that corresponds to a signal-to-noise ratio of 7 dB [25], [11]. At high signal-to-ratios, that is, for low bit error rates, nearly no loss due to the neglected estimation of noise power can be observed.

## III. Turbo-coded Modulation

### A. Transmitter

Forward error correction (FEC) coding such as turbo and convolutional coding described in the previous sections enlarge the bandwidth of the transmitted signal by a factor $1/R_c$. For strictly band-limited channels or applications prohibiting any bandwidth expansion it is necessary to use bandwidth-efficient modulation schemes. Since the late sixties Ungerboeck's Trellis Coded Modulation (TCM) is a well-known means for combining FEC coding and bandwidth-efficient modulation. Concerning the application in broadband systems such as DS-CDMA systems the question arises whether it is advantageous to save bandwidth for DS spreading by employing coded modulation schemes in order to obtain good correlation properties and hence good interference suppression instead of spending bandwidth to FEC coding.

A first approach combining turbo codes with a multilevel modulation scheme is presented in [10]. The structure of this approach is illustrated in Figure 4. Due to the desired high spectral efficiency only constituent codes of rate $R_{c1} = R_{c2} = 1/2$ are used. Here, $m'$ unpunctured code words $\mathbf{c}(k)$ of the turbo encoder shown in Figure 1 consisting of 3 bits are arranged in a parallel manner separating the systematic information bits $\mathbf{d}$ and the redundancy bits $\mathbf{c}_1$ and $\mathbf{c}_2$ of the constituent codes $C_1$ and $C_2$, respectively. After puncturing the $2m'$ redundancy bits, the resulting $(m-m')$-tuple $\mathbf{c}'$ is combined with $m'$ information bits to an $m$-tuple $\mathbf{u}(l)$ selecting one of $M = 2^m$ possible symbols.

Concerning the mapping of $\mathbf{u}(l)$ to a specific symbol $s(l)$, Figure 6 illustrates that Gray coding offers a gain of more than 2 dB over Ungerboeck's Set Partitioning [9] for coded 8-PSK. The latter mapping rule is not suited for this approach because it neglects the code structure [11]. It is rather advantageous to perform Gray encoding ensuring that the binary representations of neighboring symbols differ in 1 bit only (see Figure 5). This results in a higher average signal-to-noise-ratio after soft-output demodulation (see section III-B), and consequently, in a lower bit error rate after decoding [11]. These results might differ for other signal constellations such as QAM.

[1]This holds for the constituent codes with a constraint length of $L_c = 5$ given in Table I.

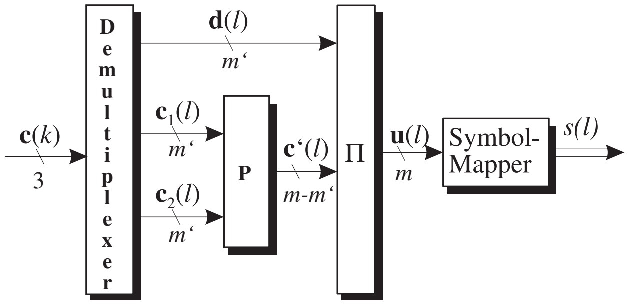


Fig. 4. Combination of turbo-encoder and modulator

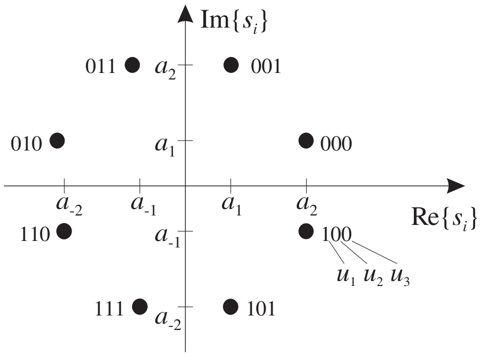


Fig. 5. Signal constellation for 8-PSK and Gray-coding

Another question affects the mapping of specific bits $c_i$ of a code word $\mathbf{c}$ to bits $u_j$ of a symbol $s(l)$. Obviously, $u_1$ and $u_2$ possess a lower error probability than $u_3$. To be exact, $P_{err}(u_3)$ is twice as high as $P_{err}(u_1) = P_{err}(u_2)$. In the case of a coded 8-PSK modulation with $R_c = 2/3$, there exist only two different possibilities concerning the mapping. In Figure 6, the configuration labeled with 'System 1' assigns both information bits of a symbol to bits $u_1$ and $u_2$ whereas the redundancy bit is mapped to the most unreliable bit $u_3$. In contrast to this, configuration 'System 2' assigns the information bits to $u_2$ and $u_3$.

Simulation results indicate that the configuration labeled with 'System 1' performs significantly better. It gains 0.3 dB over 'System 2' if Gray encoding is used. Otherwise, the difference is even higher. Generally, we can state that all bits processed directly by the *inner* decoder $D_1$ should be assigned to the most reliable bits [11]. Using this strategy, the signal-to-noise ratio at the output of the *inner* decoder is higher leading to a lower error rate after the whole decoding procedure. This behavior is caused by the iterative decoding process and is expected not to occur in the case of maximum likelihood decoding of the entire

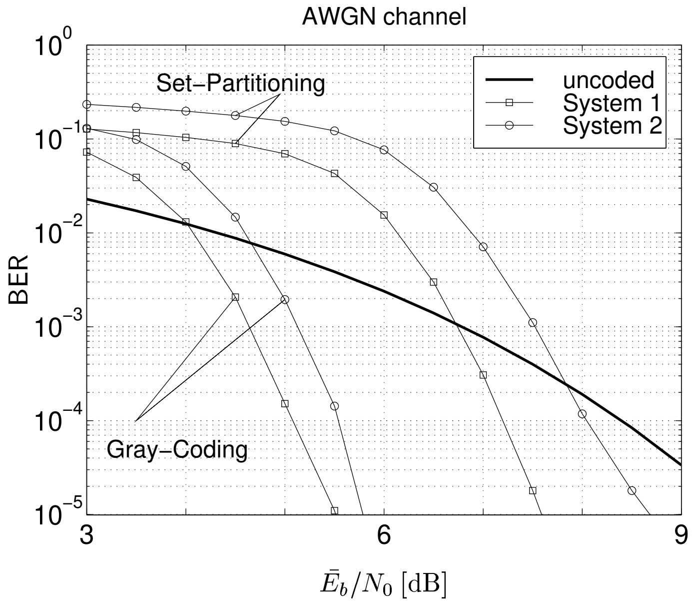

Fig. 6. Bit error rate for turbo-coded 8-PSK with different mapping for an AWGN channel

turbo code.

*B. Receiver*

The separation of encoder and modulator at the transmitter site results in separate demodulation and decoding procedures at the receiver as well as shown in Figure 7. Therefore, soft-output demodulation is required to avoid an information loss after demodulation. A straight forward realization uses the log-likelihood-ratio (LLR) that is known to be an appropriate reliability information [22].

$$\begin{aligned} L(u_j) &= \ln \frac{P(u_j=1|x)}{P(u_j=0|x)} \\ &= \ln \frac{P(x|u_j=1)}{P(x|u_j=0)} + \underbrace{\ln \frac{P(u_j=1)}{P(u_j=0)}}_{=0} \\ &= \ln \frac{\sum\limits_{s^i \in \mathcal{S}(u_j=1)} P(x|s^i)}{\sum\limits_{s^i \in \mathcal{S}(u_j=0)} P(x|s^i)} \end{aligned} \tag{10}$$

In (10), $\mathcal{S}$ represents the signal space consisting of $M$ symbols $s^i$. Depending on the specific bit $u_j$ the signal space is divided into 2 sets ($\mathcal{S}(u_j=1)$ and ($\mathcal{S}(u_j=0)$) corresponding to $u_j=1$ and $u_j=0$, respectively. For an AWGN channel and a frequency non-selective Rayleigh fading channel, the LLR is expressed by

$$L(u_j) = \ln \sum_{s^i \in \mathcal{S}(u_j=1)} e^{-\frac{|x-\alpha s^i|^2}{2\sigma^2}} - \ln \sum_{s^i \in \mathcal{S}(u_j=0)} e^{-\frac{|x-\alpha s^i|^2}{2\sigma^2}} \tag{11}$$

where $\alpha$ denotes the complex valued fading coefficient.

The application of the well-known approximation [23]

$$\ln \sum_i e^{x_i} \approx \max_i x_i \tag{12}$$

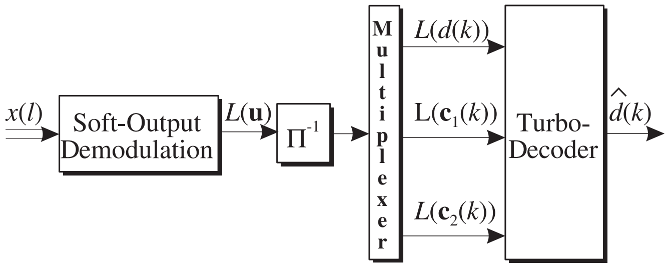

Fig. 7. Combination of demodulator and turbo-decoder

yields a simplified way of calculating soft output values

$$\begin{aligned} L(u_j) &= \max_{s^i \in \mathcal{S}(u_j=1)} -\frac{|x-\alpha s^i|^2}{2\sigma^2} - \max_{s^i \in \mathcal{S}(u_j=0)} -\frac{|x-\alpha s^i|^2}{2\sigma^2} \\ &= \min_{s^i \in \mathcal{S}(u_j=0)} \frac{|x-\alpha s^i|^2}{2\sigma^2} - \min_{s^i \in \mathcal{S}(u_j=1)} \frac{|x-\alpha s^i|^2}{2\sigma^2}. \end{aligned} \tag{13}$$

Equation (13) indicates that $L(u_j)$ depends only on the minimum Euclidean distances between the received symbol $x$ and all symbols $s^i$ corresponding to $u_j=1$ or $u_j=0$, respectively. Incorporating the coordinates $a_1$ and $a_2$ depicted in Figure 5 and using the abbreviations $x' = \mathrm{Re}\{\alpha^* x\}$ and $x'' = \mathrm{Im}\{\alpha^* x\}$ we get the following expression for an 8-PSK modulation

$$L(u_1) = \frac{-1}{\sigma^2} \begin{cases} 2a_1 \cdot x'' & |x'| \geq |x''| \\ (a_1+a_2)x'' & \\ -(a_2-a_1)|x'|\mathrm{sgn}(x'') & \text{otherwise} \end{cases} \tag{14}$$

$$L(u_2) = \frac{-1}{\sigma^2} \begin{cases} 2a_1 x' & |x'| \leq |x''| \\ (a_1+a_2)x' & \\ -(a_2-a_1)|x''|\mathrm{sgn}(x') & \text{otherwise} \end{cases} \tag{15}$$

$$L(u_3) = \frac{-1}{\sigma^2}(a_2-a_1)\left[|x'| - |x''|\right]. \tag{16}$$

Assuming that the difference $(a_2-a_1)$ is negligible compared with the sum $(a_1+a_2)$, we find a new very simple approximation

$$L(u_j) = \frac{-1}{\sigma^2} \begin{cases} 2a_1 x'' & j=1 \\ 2a_1 x' & j=2 \\ (a_2-a_1)(|x'|-|x''|) & j=3\,. \end{cases} \tag{17}$$

This expression can be easily extended for modulation schemes of higher orders. There is nearly no additional effort in supplying reliability information because only the real part and the imaginary part of the received symbol have to be detected. The conjugate complex coefficient $\alpha^*$ indicates the coherent detection at the receiver. A further motivation for this approach becomes obvious by considering the log-likelihood values that are depicted in Figure 8 and calculated by the MAP-algorithm. Obviously, there is a high degree of symmetry due to the symmetric arrangement of symbols in the signal space as illustrated in

Figure 5 [11]. Exploiting this symmetry leads to the **pragmatic approach** in (17) where $L(u_1)$ depends only on the imaginary part of $\alpha^* x$, $L(u_2)$ on the real part and $L(u_3)$ on the difference of the absolute values of both as already indicated in (17). Furthermore, it can be seen from (17) and Figure 8 that $L(u_1)$ and $L(u_2)$ are almost twice as high as $L(u_3)$ indicating that $u_3$ possesses a error probability twice as high as the other bits of a symbol.

Simulation results shown in Figure 9 illustrate only slight differences between the optimal MAP-demodulation [10],[11] and the pragmatic approach of (17) for 8-PSK modulation. In the case of 16-PSK modulation (not shown in Figure 9) the difference increases to approximately 0.3 dB due to the higher density in signal space. In contrast to hard-decision decoding (labeled with 'HD') a gain of 3 dB for the AWGN channel and of more than 6 dB for the fully-interleaved flat Rayleigh fading channel is obtained.

A further simplification was achieved by replacing the estimated noise variance $\sigma^2$ by a constant value of $\sigma^2 \equiv 0.1$ leading only to a minor performance loss. Using this approach, nearly no additional costs are required to supply soft-output information. Additionally, the interpretation of $L\{u_j\}$ as a log-likelihood-ratio reduces the computational costs of the decoding algorithms. Following the concept in [23], no estimation of the noise variance is necessary.

## IV. CDMA Simulation Model

The last sections presented the principle of turbo codes, a guideline for choosing good constituent codes, an approach for combining turbo codes with multi-phase modulation schemes and a very simple soft-output demodulation algorithm. In order to verify the performance of these methods in comparison with conventional coding techniques, they are now embedded in a mobile radio system based on the CDMA multiplex technique. Figure 10 shows the structure of the simulation model. The data stream $d(k)$ of rate of $R_d$ =9.6 kbit/s is first encoded by the channel encoder employing conventional convolutional codes (CC) or turbo codes (TC) as described above. After interleaving the code words $\mathbf{c}(k)$, they are mapped to PSK-symbols $s(l)$. Direct-Sequence spreading is performed separately for inphase and quadrature component using Gold Codes of periods 31, 63 and 127.

As shown in Table II, different parameter configurations are applied in order to find a good compromise between DS-spreading and channel coding. In the case of an uncoded transmission the bandwidth is increased by a factor 127 solely by DS-spreading. By applying channel coding, this bandwidth expansion is reduced by a factor equal to the code rate $R_c$. As a consequence, all system configurations maintain approximately the same processing gain of $G_P \approx 63$.

As applied in the down-link of the QUALCOMM-system, an unmodulated pilot signal is added. It possesses a power 6 dB higher than the power of the data signals to ensure synchronization. Furthermore, it is used for channel estimation once per symbol duration [26], [11]. The mobile radio channel is modeled as a four-path Rayleigh fading channel with a maximum Doppler frequency shift of $f_{d\,max} = 200$ Hz at a carrier frequency of $f_0 = 900$ MHz. In order to spread bursty errors into single errors channel interleavers with dimensions shown in Table II are used. The specific number of rows depends on the code rate and the constraint length of the actual code. For the convolutional code as well as for turbo codes $a = L_c/R_c$ rows is a good choice. Depending on $a$, the number of columns $b$ was determined in a way to obtain the same total delay for all configurations. The turbo code with its inherent interleaver of 20 rows and 20 columns causes a total transmission delay of 83 ms. Concerning the code rate $R_c = 1/2$ this delay is not increased by a channel interleaver with $a = L_c/R_c = 10$ rows and $b = 80$ columns. The corresponding interleaver for the convolutional code has the dimension of 18 rows and 45 columns. This choice results in a time spacing between two successive bits of $\Delta t = 2.34$ ms that suffices for a coherence time of the channel of $t_c = 2.5$ ms.

TABLE II
Parameter configuration

| Modulation | Channel interleaver | DS-Spread | $G_P$ |
|---|---|---|---|
| QPSK | uncoded | 127 | 63.5 |
| QPSK $R_c = 1/2$ | CC: 18x45 TC: 10x80 | 63 | 63 |
| QPSK $R_c = 1/4$ | CC: 36x45 TC: 20x80 | 31 | 62 |
| 8-PSK $R_c = \frac{2}{3}$ | TC: 10x60 | 127 | 63.5 |

## V. Simulation Results

This paper pursues two goals: First, turbo codes are to be compared with convolutional codes under the constraint of approximately the same computational decoding effort and small turbo code interleavers. Second, a compromise between a high coding gain (low code rate) and high Direct-Sequence spreading should be worked out. A high DS spreading factor ensures better correlation properties and thus yields a better suppression of interference due to multi-path propagation and multi-user interference. This advantage is attached with a high code rate and consequently a small coding gain.

Figure 11 illustrates the bit error rates for convolutional codes, turbo codes and turbo-coded modulation for different code rates. Concerning the convolutional codes, no differences for 1/2-rate and 1/4-rate coding can be observed. The Turbo-Code with rate 1/4 performs as well as the latter ones, whereas the rate 1/2-Turbo-Code has a lower performance. Other authors in [27],[28],[29] presented results where the performance of turbo codes is slightly better than the one of a constraint length $L_c = 5$ CC depending

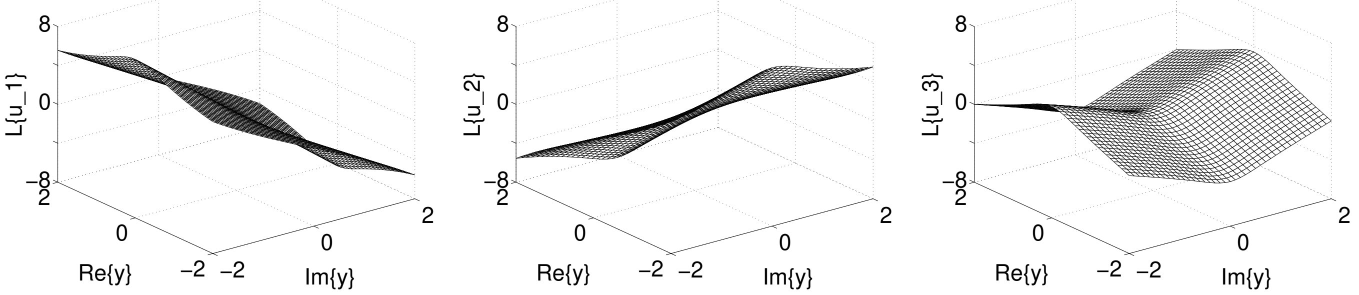


Fig. 8. Log-likelihood ratios of MAP demodulation

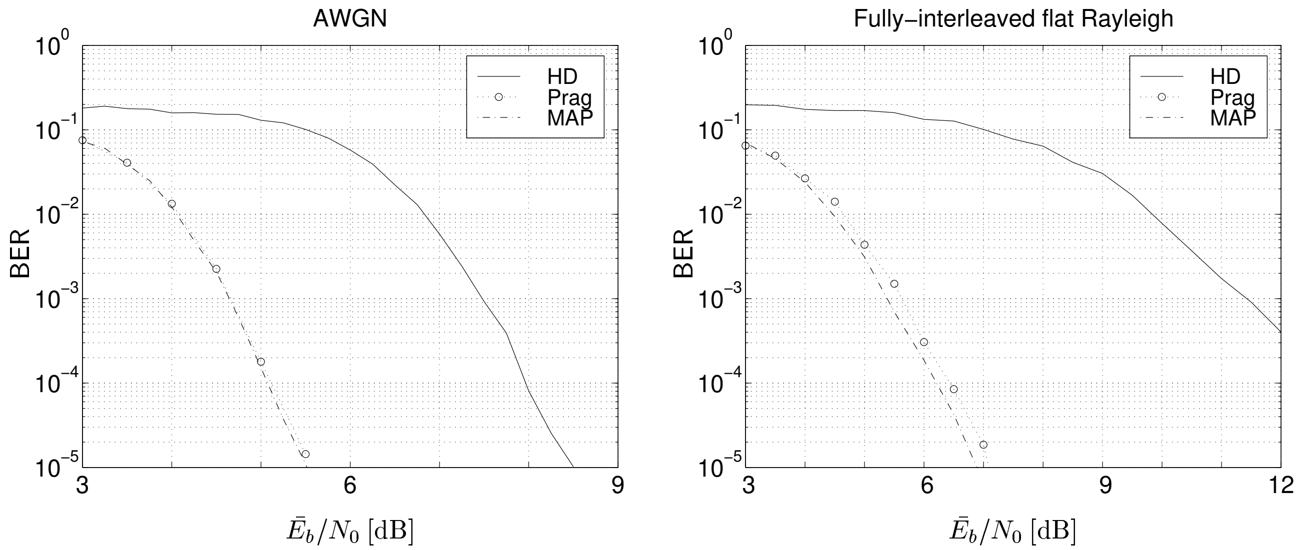


Fig. 9. Bit error rates for different soft-output demodulation algorithms for AWGN and fully-interleaved frequency non-selective Rayleigh fading channel

on the specific channel model. Although a comparison to these results is somewhat difficult due to different system configurations, these results may support our conclusion that the turbo codes considered in this paper and a CC with $L_c = 9$ have approximately the same performance. The convolutional code with constraint length $L_c = 9$ was chosen in order to ensure only twice as high decoding costs.

The turbo-coded 8-PSK loses up to 1 dB over the other configurat caused by a higher signal density in combination with a lower coding gain. Moreover, the 8-PSK modulation is more sensitive to phase shifts due to the fading process. These disadvantages cannot be compensated by better correlation properties of high DS spreading [11].

Surprisingly, only a small difference between code rates of $R_c = 1/4$ and $R_c = 1/2$ occurs. In order to investigate this effect in more detail, we found that the accuracy of the channel estimation has a significant influence on the coding gain. Although the pilot signal is transmitted with a higher power in comparison with the data signals, the signal-to-noise-ratio is still too low for an accurate estimation. A better suppression of the background noise can be achieved by averaging e.g. ten estimated channel coefficients [11]. For a maximum Doppler frequency of $f_{d\,max} = 200$ Hz - this corresponds with a coherence time of the channel of $\Delta t_c = \frac{1}{2 \cdot f_{d\,max}} = 2.5$ ms - the channel is nearly time-invariant for a duration of ten symbols ($\approx 1$ ms). This holds even for a carrier frequency of $f_0 \approx 2$ GHz doubling the maximum Doppler frequency. For channels fading much faster than $f_{d\,max} = 400$ Hz further investigations have to be carried out.

An illustration is given in Figure 12 depicting the bit error rates for perfectly known channel coefficients, non-averaged and averaged estimated coefficients. Concerning the latter approach 10 estimated coefficients were averaged. Obviously, the accuracy of the channel estimation strongly determines the performance of channel coding. Averaging ten estimated values leads to a gain of 3 dB over the non-averaged estimation, there remains only a loss of 1 dB over perfectly known coefficients.

Additionally, a code rate of 1/4 with a spreading sequence of length 31 now outperforms the code with rate 1/2 and a spreading sequence with period 63 by 1 dB at a BER of $10^{-4}$. These results lead to the conclusion that the advantages of powerful channel codes with low code rate can only be exploited by an accurate estimation of the channel state. The difference between perfectly known coefficients and conventional estimation for the coded 8-PSK modulation is only 1 dB, so additional averaging will not

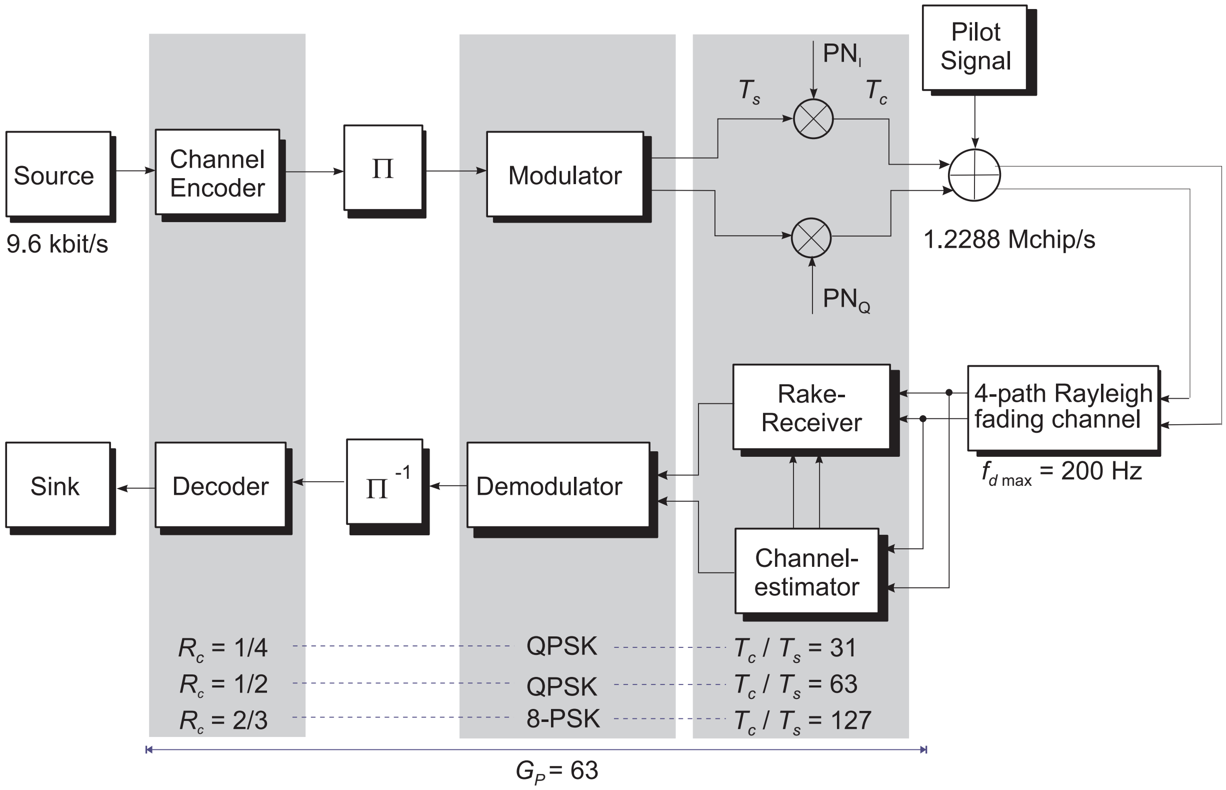


Fig. 10. Structure of CDMA system model

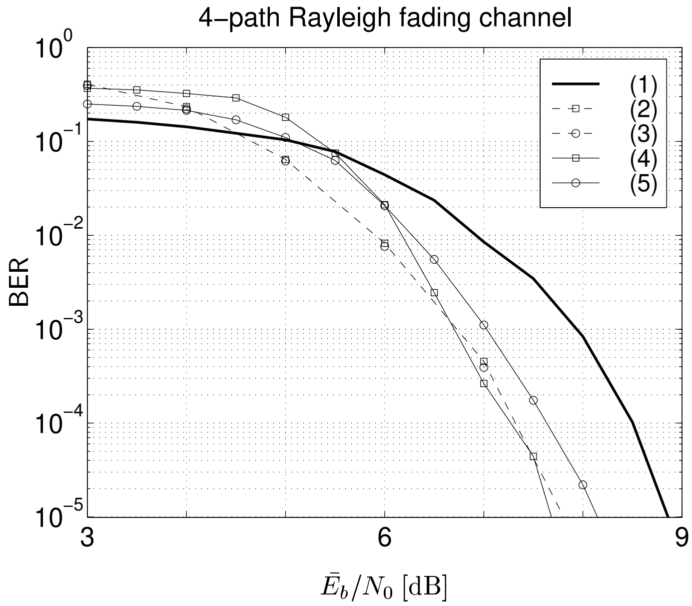


Fig. 11. Bit error rates for a 4-path Rayleigh fading channel and different coding scenarios, (1) TC-8-PSK with $R_c = 2/3$, (2) CC with $R_c = 1/4$, (3) CC with $R_c = 1/2$, (4) TC with $R_c = 1/4$, (5) TC with $R_c = 1/2$

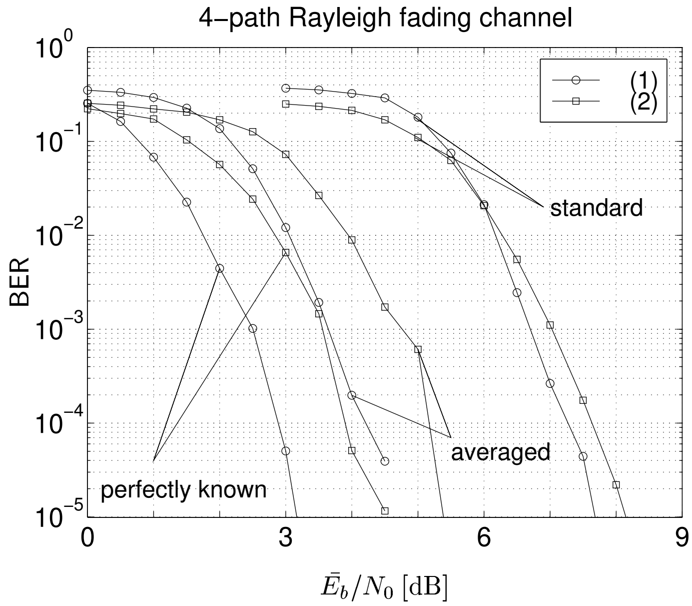


Fig. 12. Bit error rate for perfectly known and estimated channel coefficients and turbo codes, (1) TC with $R_c = 1/4$, (2) TC with $R_c = 1/2$

result in large gains and is therefore not considered here.

Finally, the performance is checked under the consideration of ten additional users causing multi-user interference. Additional users have been explicitely simulated and were not considered by the gaussian approximation. As can be seen in Figure 13, the difference between rate 1/4 and rate 1/2 coding is reduced. The longer Gold-sequence of length 63 (s. Table II) ensures a better estimation of the channel and a better suppression of additional interfering user signals. Concerning the coded 8-PSK the unsatisfying performance is obvious.

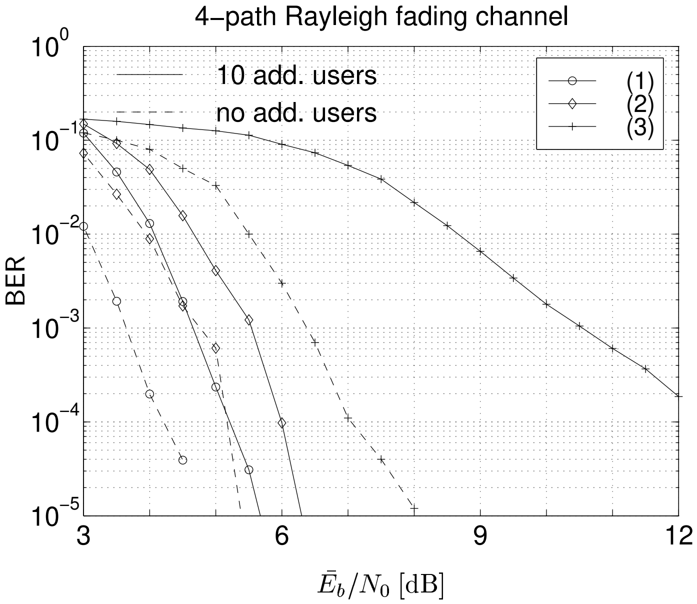


Fig. 13. Bit error rate for additional users and turbo codes, dashed lines: no additional users, solid lines: 10 additional users, (1) TC with $R_c = 1/4$, (2) TC with $R_c = 1/2$, (3) TC-8-PSK with $R_c = 2/3$

## VI. Conclusion

Concerning the specific conditions underlayed in this paper turbo codes are not superior to convolutional codes. One reason is the use of simple block interleavers and the restriction of the interleaver size to 400 bits allowing an application for speech transmission. In contrast to other publications, turbo codes have been compared with powerful convolutional codes of constraint length $L_c = 9$. Nevertheless, optimizing the turbo code, e.g. by an advanced interleaver structure, will lead probably to a performance improvement but the advantage is expected to be small for short interleavers. Furthermore, the turbo-coded 8-PSK modulation described here is not attractive in a spread spectrum system. It is rather advantageous to decrease the code rate and to shorten the DS-spreading. In order to take advantage of more powerful codes, an accurate channel estimation is necessary. This can be realized by averaging an appropriate number of estimated channel coefficients leading to a performance gain up to 3 dB. Additional simulations have to be carried out in order to corroborate the presented results for different interleaver sizes and maximum Doppler frequencies.

## References


[1] C. Berrou, A. Glavieux, and P. Thitimajshima, "Near Shannon limit error-correcting coding and decoding: Turbo codes", in *IEEE Int. Conf. on Communications*, 1993, pp. 1064–1070.

[2] G. D. Forney, *Concatenated Codes*, The M.I.T. Press, Cambridge, Massachusetts, 1966.

[3] P. Hoeher, "New iterative "turbo" decoding algorithms", in *Int. Symp. on Turbo Codes and Related Topics*, 1997, pp. 63–70.

[4] Patrick Robertson, Emmanuelle Villebrun, and Peter Hoeher, "A comparison of optimal and sub-optimal MAP decoding algorithms operatiting in the log domain", in *IEEE Int. Conf. on Communications*, 1995, pp. 1009–1013.

[5] P. Jung, "Comparison of turbo-code decoders applied to short frame transmission", *IEEE Jour. of Sel. Areas in Communications*, pp. 530–537, Apr. 1996.

[6] P. Jung, "Novel low complexity decoder for turbo codes", *Electronics Letters*, pp. 86–87, Jan. 1995.

[7] X. Li, B. Vucetic, and Y. Sato, "Optimum Soft-Output Detection for Channels with Intersymbol Interference", *IEEE Transactions on Information Theory*, vol. 41, no. 3, pp. 704–713, May 1995.

[8] C. Douillard, M. J´ez´equel, and C. Berrou, "Iterative Correction of Intersymbol Interference: Turbo-Equalization", *European Transactions on Telecommunications ETT*, vol. 6, 1995.

[9] G. Ungerboeck, "Channel Coding with Multilevel Phase Signaling", *IEEE Transactions on Information Theory*, vol. IT-25, pp. 55–67, 1982.

[10] S. Le Goff, A. Glavieux, and C. Berrou, "Turbo-Codes and High Spectral Efficiency Modulation", in *Proc. IEEE International Conference on Communications (ICC'94)*, New Orleans, 1994, pp. 645–649.

[11] V. Kuehn, *Turbo-Codes und turbo-codierte Modulation in Codemultiplex-Mobilfunksystemen*, PhD thesis, University of Paderborn, 1998.

[12] P. Robertson and T. Wörz, "A novel coded modulation scheme employing turbo codes", in *URSI & ITG Conference 'Kleinheubacher Tagung'*, Kleinheubach, Germany, Oct. 1995.

[13] P. Robertson and T. Woerz, "Extentions of turbo trellis-coded modulation to high bandwidth efficiencies", in *IEEE Int. Conf. on Communications*, 1997.

[14] S. Benedetto et al., "Bandwidth efficient parallel concatenated coding scheme", *Electronics Letters*, vol. 31, no. 24, pp. 2067–2069, Nov. 1995.

[15] S. Benedetto, D. Divsalar, G. Montorsi, and F. Pollara, "Parallel concatenated trellis coded modulation", in *IEEE Int. Conf. on Communications*, 1996, pp. 974–978.

[16] C. Berrou, A. Glavieux, and P. Thitimajshima, "Near Shannon Limit Error-Correcting Coding and Decoding: Turbo-Codes (1)", in *Proc. IEEE International Conference on Communications (ICC'93)*, Geneva, 1993, pp. 1064–1070.

[17] S. Benedetto and G. Montorsi, "Unveiling turbo codes: Some results on parallel concatenated coding schemes", *IEEE Tran. on Information Theory*, vol. 42, no. 2, pp. 409–429, Mar. 1996.

[18] S. Benedetto and G. Montorsi, "Design of parallel concatenated convolutional codes", *IEEE Tran. on Communications*, vol. 44, no. 5, pp. 591–600, May 1996.

[19] L. Perez, J. Seghers, and D. Costello, "A distance spectrum interpretation of turbo codes", *IEEE Tran. on Information Theory*, vol. 42, pp. 1698–1709, November 1996.

[20] J. G. Proakis, *Digital Communications*, McGraw-Hill, third edition, 1995.

[21] L.C. Perez, J. Seghers, and D.J. Costello, "A Distance Spectrum Interpretation of Turbo Codes", *IEEE Transactions on Information Theory*, vol. 42, no. 6, pp. 1698–1709, November 1996.

[22] J. Hagenauer, P. Robertson, and L. Papke, "Iterative (Turbo)-Decoding of Systematic Convolutional Codes with the MAP and SOVA Algorithms", in *Proc. ITG Fachtagung'Codierung', Munich (Germany)*, October 1994, pp. 21–29.

[23] P. Robertson, E. Villebrun, and P. Hoeher, "A Comparison of Optimal and Sub-Optimal MAP Decoding Algorithms Operating in the Log Domain", in *International Conference on Communications (ICC'95)*, June 1995.

[24] P. Jung, "Comparison of Turbo-Code Decoders Applied to Short Frame Transmission Systems", *IEEE Journal on Selected Areas in Communications*, vol. 14, no. 3, pp. 530–537, April 1996.

[25] Todd Summers and Stephen G. Wilson, "Snr mismath and online estimation in turbo decoding", To appear IEEE Trans. on Communications, 1997.

[26] V. Kuehn and M. Meyer, "Correlative Channel Estimation in DS-CDMA Systems", in *Third Annual WIRELESS Symposium*. 1995, pp. 279–284, Penton Publishing.

[27] P. Jung, M. Nasshan, and J. Blanz, "Application of Turbo-Codes to a CDMA mobile radio system using joint detection and antenna diversity", in *Proceedings of the IEEE 44th Vehicular Technology Conference VTC-94*, Stockholm, 1994, pp. 770–774.

[28] M. Nasshan and P. Jung, "New results on the application of antenna diversity and Turbo-Codes in a JD-CDMA mobile radio system", in *Proceedings of the Fifth International Symposium*

*on Personal, Indoor and Mobile Radio Communications (PIMRC'94)*, The Hague, 1994, pp. 524–528.

[29] P. Jung and M. Nasshan, "Applying Turbo-Codes to the uplink in a JD-CDMA mobile radio system using coherent receiver antenna diversity", in *Proceedings of the ITG Conference Source and Channel Coding*, Munich, 1994, pp. 49–56.

**Volker Kühn was born in Paderborn, Germany, in 1966. He received the M.Sc. degree in electrical and electronics engineering from the University of Paderborn in 1993. From 1994 to 1998 he was with the Department of Communications Engineering at the University of Paderborn where he received the Ph.D. degree in 1998. Currently, he is with the Department of Telecommunications at the University of Bremen. His main fields of interest are channel coding, iterative decoding, modulation as well as CDMA.**